Theor Appl Genet (2006) 113:1395–1407
DOI 10.1007/s00122-006-0359-2

ORIGINAL PAPER

Quantitative trait loci analysis of phenotypic traits and principal components of maize tassel inflorescence architecture

N. Upadyayula · J. Wassom · M. O. Bohn · T. R. Rocheford

Received: 11 January 2006 / Accepted: 30 June 2006 / Published online: 24 October 2006

Abstract Maize tassel inflorescence architecture is relevant to efficient production of F_1 seed and yield performance of F_1 hybrids. The objectives of this study were to identify genetic relationships among seven measured tassel inflorescence architecture traits and six calculated traits in a maize backcross population derived from two lines with differing tassel architectures, and identify Quantitative Trait Loci (QTL) involved in the inheritance of those tassel inflorescence architecture traits. A Principal Component (PC) analysis was performed to examine relationships among correlated traits. Traits with high loadings for PC1 were branch number and branch number density, for PC2 were spikelet density on central spike and primary branch, and for PC3 were lengths of tassel and central spike. We detected 45 QTL for individual architecture traits and eight QTL for the three PCs. For control of inflorescence architecture, important QTL were found in bins 7.02 and 9.02. The interval phi034—*ramosa1* (*ral*) in bin 7.02 was associated with six individual architecture trait QTL and explained the largest amount of phenotypic variation (17.3%) for PC1. Interval bnlg344–phi027 in bin 9.02 explained the largest amount of phenotypic variation (14.6%) for PC2. Inflorescence architecture QTL were detected in regions with candidate genes *fasciated ear2, thick tassel dwarf1*, and *ral*. However, the vast majority of QTL mapped to regions without known candidate genes, indicating positional cloning efforts will be necessary to identify these genes.

Communicated by T. Lübberstedt.

N. Upadyayula (✉) · J. Wassom · M. O. Bohn · T. R. Rocheford
Department of Crop Sciences, University of Illinois, Urbana, IL 61801, USA
e-mail: upadyayu@uiuc.edu

Introduction

Maize (*Zea mays* L.) is a monoecious, naturally outcrossing species. The historical change from growing open pollinated varieties to single cross F_1 hybrids required creation of large quantities of two parental inbreds that are crossed to create sufficient F_1 seed for planting extensive acreages. This process generally involves planting adjacent blocks of four rows of an inbred that is used as female to produce seed and two rows of a male that serves as pollinator (Wych 1988). The female plants are detasseled or are male sterile and ideally produce large amounts of high-quality seed. The desirable male parent has a tassel with an intermediate tassel branch angle (TBA) to facilitate pollen dispersal, and preferably not a very upright TBA. The male parent should produce a large amount of pollen that sheds over a few days, not just a single day in order to synchronize with silk emergence on the female plant. This generally involves a tassel architecture with above average spikelet densities and number of long branches, but other architectures may be satisfactory. In contrast, the female parent preferably has a very small tassel with few or no long branches and low-spikelet densities, so that the plant does not expend much energy into production of organs that are not necessary to produce seed (Lambert and Johnson 1977).

A primary objective of maize breeders has been increasing grain yield performance of F_1 hybrids. These efforts have been successful in the last several decades, but have been associated with a reduction in the size of tassels on F_1 hybrids (Duvick and Cassman 1999). Older open pollinated varieties and early era F_1 hybrids have large, extensive tassels that shed pollen over a relatively long-period of time. In contrast, contemporary F_1 hybrids have relatively small tassels with few side branches and in some cases no side branches. The smaller tassels are likely an indirect response to selection for higher grain yields. Selection for smaller tassels reduces energy expended on the tassel and reduces shading of the flag and upper leaves (Lambert and Johnson 1977). However, smaller F_1 tassels create challenges in seed production, since the male parent needs enough branches and spikelets to produce sufficient pollen to successfully pollinate the female parent. Furthermore, some female parent inbreds have such small tassels that they have become difficult to maintain in the breeding nursery, as they may shed pollen only for one day. These contrasting needs creates conflicting challenges for plant breeders that wish to maximize grain yield on F_1 hybrids and seed production managers that wish to maximize the economic production of F_1 hybrid seed (Wych 1988). In some cases an inbred used as a male may be associated with high-grain yield potential in F_1 hybrids but not used as a parent because it does not produce enough pollen. Thus more information on genetic control of maize tassel inflorescence architecture that may enable rapid manipulation of inflorescence architecture in advanced breeding materials may help address these contrasting needs.

Research efforts on maize inflorescence architecture have identified numerous mutants (Neuffer et al. 1997), which provide information on how single genes can affect inflorescence architecture, with some mutants affecting more than one component of inflorescence architecture. A number of genes associated with these mutants (McSteen et al. 2000) have been cloned through transposon tagging and recently through positional cloning (Bortiri et al. 2006). The mutants provide useful resources for identifying candidate genes underlying Quantitative Trait Loci (QTL) (Robertson 1985), and cloned genes enable association analysis tests (Wilson et al. 2004) to assess relationship of the gene and quantitative variation in relevant traits. Successful association tests will enable identification of favorable alleles that can be efficiently used for allele specific introgression and selection. These alleles could be used to rapidly alter inflorescence architecture and make a line more suitable as a male or female parent. However, there are a large number of QTL identified in previous studies (Berke and Rocheford 1995; Mickelson et al. 2002; Upadyayula et al. 2006) that do not map to mutants and cloned genes. Therefore, QTL mapping approaches, which identify loci with no known relevant mutants or cloned genes, provide useful initial mapping information for new gene discovery efforts. With the present initiative to sequence the maize genome (MaizeGDB 2006), inflorescence architecture QTL information will be useful for positional cloning of the underlying genes.

The experimental design in QTL mapping studies usually involves measurements of numerous traits, many of which are correlated. In most cases QTL analysis is done trait-by-trait. However, using multivariate approaches, by taking into account the correlation structure between traits, may increase the power of QTL detection and will improve the understanding of the genetic basis of trait correlations (Jiang and Zeng 1995). Multivariate analysis for multitrait QTL detection has been proposed by some authors (Jiang and Zeng 1995; Korol et al. 1995; Weller et al. 1996; Knott and Haley 2000; Gilbert and LeRoy 2003). Multivariate analysis, besides being statistically more appropriate may assist in testing several biologically important hypotheses, e.g., to distinguish between linkage and pleiotropy as mechanisms of genetic correlations, or to address the problem of QTL by environment interactions (Jiang and Zeng 1995). In this study, we used principal component analysis (PCA), one of the most widely used multivariate methods, to detect QTL associated with sets of tassel architectural traits.

The central purpose of PCA is to reduce the dimensionality of a data set consisting of a large number of correlated variables, while retaining as much as possible of the variation present in the data set (Jolliffe 1986). This is achieved by identifying uncorrelated linear combinations of traits, the Principal Components (PCs), which are derived from the components of the eigenvectors of the phenotypic covariance or correlation matrix. The PC scores are calculated for each experimental unit by applying characteristic linear combination of traits as indicated by the respective eigenvector. Thus PCs can be considered as new uncorrelated traits and could be subjected to genetic analyses and QTL can be identified underlying their inheritance. PC analysis was used in this study to dissect genetic networks that regulate tassel architecture and to increase the power of QTL detection by reducing multiple hypothesis testing concerns by combining a large set of correlated traits into fewer PCs. PCA is appropriate for tassel architecture

data, where most of the traits are correlated (Upadyayula et al. 2006). The QTL for PCs potentially may reveal loci that are more efficient and effective in marker assisted selection efforts to rapidly alter inflorescence architecture phenotypes than conventional QTL revealed by single trait analysis.

The objectives of this study were to identify (1) genetic relationships between a comprehensive set of tassel inflorescence architecture traits evaluated in a set of BC_1 derived S_1 lines (BC_1S_1) lines derived from maize cultivars with contrasting tassel characteristics and (2) QTL involved in their inheritance using univariate and multivariate approaches.

Materials and methods

Genetic materials

Backcross-derived lines were produced from Illinois High Oil (IHO) and inbred B73. Inbred B73 is a historically important, publicly available inbred line in the pedigree of many production-oriented inbreds. B73 has a relatively small tassel with few branches and lower spikelet densities. The IHO selection strain was developed by recurrent selection for high-oil content (Dudley and Lambert 1992, 2004; Lambert 2001) and has large, highly branched tassels with above average spikelet densities (Berke and Rocheford 1995). IHO was selected as a parent as it likely has alleles that could increase inflorescence architecture traits in a B73 background.

The IHO donor was a single randomly chosen plant from IHO cycle 90. IHO cycle 90 has a relatively high-inbreeding level with an inbreeding coefficient of > 0.82 (Dudley et al. 1974). The IHO90 plant was crossed with B73 to produce IHO90 $\times$ B73 F_1. A single random F_1 plant was then backcrossed with B73 to produce BC_1 generation. BC_1 progeny from a single ear were self pollinated to produce 150 BC_1S_1 lines each line traceable to a single BC_1 plant. Plants within these families were sibmated to produce enough seed for replicated field evaluation. A sample of the IHO90 strain and the B73 inbred were used in the experiments as parental checks.

Field evaluations

Field trials were conducted at the University of Illinois Research and Education Center in Urbana, IL. The experiments were grown in two replicates in 1996, 2001–2003, and included 150 BC_1S_1 lines along with ten checks, which included the parental lines as single entries. Each replicate was randomized as an 32×5 α (0,1) design. The 160 lines were grown in one-row nursery plots, 4.6 m long and 0.76 m apart. Plots were thinned to 15 plants/row (equivalent to 43,000 plants/ha).

Phenotypic evaluations

Following completion of pollen shed in the plots, average TBA was visually estimated on 2–3 representative tassels for each plot, where 0° corresponds to side branches perpendicular to the central spike and 90° corresponds to side branches parallel to the central spike. After angle estimates were taken, five random tassels were harvested from each plot. These samples were placed in bags and dried in an outdoor forced-air dryer at approximately 40°C. A set of measurements were recorded for each dried tassel: total tassel length (L1), central spike length (L2), tassel branch number (TBN), and tassel weight (TW). The number of spikelet pairs was recorded from a 4 cm segment of the central spike and a 6 cm segment of the lowest side branch. Branch zone length (L3), and total spikelet pairs on central spike were calculated from the measured traits. Several ratios were calculated from this data, further details regarding measurement and calculation of traits are described in Table 1 and in Upadyayula et al. (2006). The terms long-branch meristem and short-branch meristems refer to the meristems that give rise to tassel branches and spikelets, respectively.

Phenotypic data analyses

Best linear unbiased predictors (BLUPs) of plot means for all traits across the years were calculated using the model: $y_{ijkl} = \mu + \alpha_i + \beta_{j(i)} + \delta_{k(ij)} + \gamma_l + (\gamma\alpha)_{il} + \varepsilon_{ijkl}$, where y_{ijkl} represents the phenotypic mean of a line, α_i the effect of ith year, $\beta_{j(i)}$ the effect of jth replication in the ith year, $\delta_{k(ij)}$ the effect of kth block in jth replication of ith year, γ_l the effect of the lth line, $(\gamma\alpha)_{il}$ the effect of lth family by ith year interaction, and ε_{ijkl} represents residual error. All the effects in the model were considered random, and were performed using the SAS statistical software package (SAS Institute 2003). Estimates of variance components σ^2_g(genetic variance), σ^2_{ge} (genotype $\times$ environment interaction variance), and σ^2 (error variance) of the BC_1S_1 families and their standard errors were calculated as described by Searle (1971, p. 475), using a completely randomized design as an incomplete block design was not efficient. Heritability estimates ($\hat{h}^2$) for the BC_1S_1 families were calculated on an entry-mean basis as

Table 1 List of tassel inflorescence architecture measurements

Trait	Abbreviation	How measured/calculated
Total tassel length	L1	Measured from the non branching node present below the lowermost primary branch to the tip of central spike
Central spike length	L2	Measured from top branch to tip of central spike
Branch zone length	L3	L1–L2; the length from the top branch to the non-branching node present below the lowermost primary branch
Tassel weight	TW	Mass in g of entire dried tassel plus 2 cm from the non-branching node present below the lowermost primary branch
Tassel branch angle	TBA	Average tassel angle estimated in the field for each family; 0° = side branches are perpendicular to the central spike, 90° = side branches are parallel to the central spike
Tassel branch number	TBN	Number of primary branches
Central spike spikelet pair density	CSD	Number of spikelet pairs on top 4 cm of central spike
Primary branch spikelet pair density	PSD	Number of spikelet pairs on top 6 cm of lowermost primary branch
Total spikelets on central spike	TS	(CSD × central spike length)/4 cm
Branch number/central spike length	TBN/L2	Ratio of branch number to central spike length
Branch number density	TBN/L3	Number of branches per cm
Total spikelets on central spike/branch number	TS/TBN	Ratio of TS to branch number
Branch zone length/central spike length	L3/L2	Ratio of branch zone length to central spike length

described by Hallauer and Miranda (1988): $\hat{h}^2 = \hat{\sigma}_g^2 \Big/ \left(\hat{\sigma}_g^2 + \hat{\sigma}_{ge}^2 \Big/ e + \hat{\sigma}^2 / re\right)$, where r represents number of replications and e represents number of environments. The 90% confidence intervals on $\hat{h}^2$ were determined according to Knapp et al. (1985). Phenotypic (r_p) and genotypic (r_g) correlation coefficients were calculated among the traits based on BLUPs of BC_1S_1 families by applying standard procedures (Mode and Robinson 1959) using PLABSTAT (Utz 2001).

Principal component analysis

Principal component analysis is a linear combination of the original variables and can be done on the covariance or correlation matrix of the phenotypic data. In PCA, let $\sum$ represent the covariance or correlation matrix associated with a set of p phenotypic traits represented by a vector $X' = [X_1, X_2, ..., X_P]$ and let $\sum$ have the eigenvalue–eigenvector pairs (λ_1, e_1), (λ_2, e_2), ..., (λ_p, e_p) where $\lambda_1 \geq \lambda_2 \geq \cdots \geq \lambda p \geq 0$. Then the ith PC is given by $Yi = e'_1 \; X = e_{i1} \; X_1 + e_{i2}X_2 + \cdots + e_{ip}X_p$, where $i = 1, 2, ..., p$. The percentage of variation of the original traits explained by each PC is equal to the associated eigenvalue. We performed PCA on the phenotypic correlation matrix, obtained from the BLUPs of all traits, using procedure PRINCOMP in SAS (SAS Institute 2003). We used PCA to identify quantitative phenotypes that represent independent systems of trait variation. For each BC_1S_1 family PC scores were obtained by multiplying the eigenvector matrix with the data matrix of the standardized BLUPs. The PC scores were regarded as phenotypes and used to map QTL associated with these PCs.

Quantitative trait loci analysis

A linkage map was constructed with 102 molecular markers using JoinMap Version 3.0 (Van Ooijen et al. 2001). JoinMap data analysis tools were used to evaluate quality of molecular marker data. Data were screened for segregation distortion and similarity between markers or individuals and markers were removed for high level of segregation distortion. The final map (Fig. 1) had a total genome length of 1,133 centimorgans (cM) and an average interval length of 12.3 cM between markers. Single trait QTL mapping was based on BLUP estimates of family values across environments. The method of Composite Interval Mapping (CIM) (Jansen and Stam 1994; Zeng 1994) was employed for detecting QTL for each trait (univariately) and for the first three PCs, using PLABQTL (Utz and Melchinger 1996). The model used for QTL detection was: $y_j = a + b_i X_{ij} + \sum_{k \neq i,i+1} g_k Z_{kj} + \varepsilon_j$ where y_j represents the trait value for the individual j, a represents the intercept of the model, b_i represents the genetic effect of the putative QTL located between markers i and i+1, X_{ij} represents a dummy variable taking 1 for QTL genotype AA, 0 for Aa, g_k represents

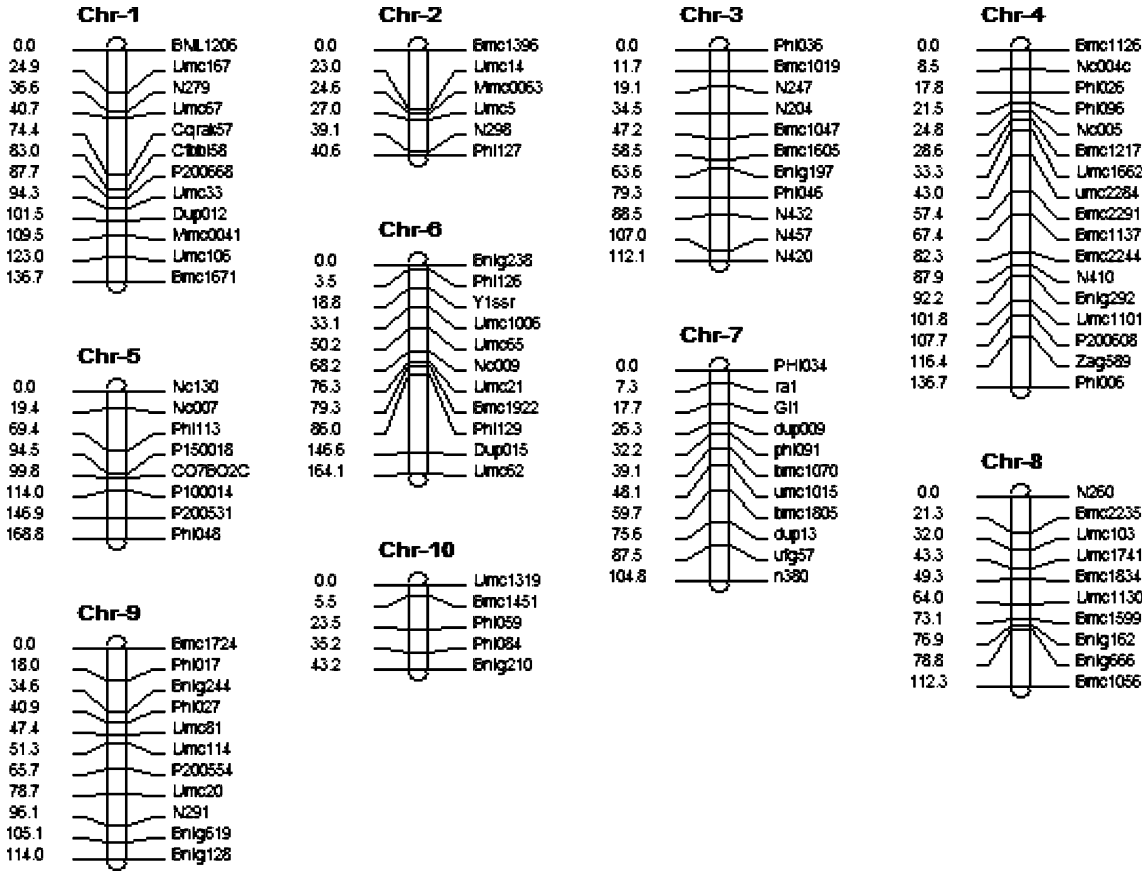

Fig. 1 Molecular map of maize backcross of (IHO × B73) B73 S_1 families

the partial regression coefficient of the trait value on marker cofactor k, Z_{kj} represents dummy variable for marker k and individual j, taking 1 if the marker has genotype AA and 0 for Aa, and ε_j is a residual from the model. Cofactors, Z_{kj} were selected for each trait by a stepwise regression procedure (Draper and Smith 1981, p307 *ff*). Final selection was for the model that minimized Akaike's information criterion with penalty = 3.0. Threshold LOD values for each trait were calculated by performing 1,000 permutations (Churchill and Doerge 1994) at a genome-wise significance level of $\alpha = 0.30$ which corresponds to a comparison-wise significance of $\alpha' = 0.0026$. LOD curves were created by scanning every 2 cM of the genome. The phenotypic variation accounted for by an individual QTL (R^2) was calculated as the square of the partial correlation coefficient from the final multiple regression model. This value is the coefficient of determination of specified QTL, the phenotypic variation explained by the QTL keeping all the other QTL detected for that trait fixed (Utz and Melchinger 1996). The proportion of phenotypic variance explained by all QTL in the model, with adjustment for the number of terms in the multiple regression models (adjusted R^2) was calculated according to Hospital et al. (1997). The percentage of total genotypic variance explained by the model (adjusted p) was calculated as adjusted R^2 divided by heritability (Dudley 1994). Quantitative trait loci for different traits were declared as potential ''common QTL'', when they were detected between the same marker interval.

Results

Phenotypic analysis

The IHO parental check showed a larger tassel than B73 with more branches (30.0 vs. 8.0), heavier tassel (8.7 g vs. 2.1 g) and central spike with higher spikelet density (34.0 spikelet pairs/4 cm vs. 27.8 spikelet pairs/4 cm) (Table 2). L1 and L2 were similar in both parents. Among the BC_1S_1 families, transgressive segregation relative to parental checks was observed only for L1, L2, and central spike spikelet density. The IHO90 strain is not completely inbred and this may influence inflorescence trait values and comparisons with the BC_1S_1 families.

Table 2 Means of parents Illinois High Oil (*IHO*) and B73, and 150 S_1 lines derived from backcross (IHO × B73) B73, along with estimates of variance components and heritabilities among BC_1S_1 families for measured traits, including total tassel length (*L1*), central spike length (*L2*), tassel branch number (*TBN*), central spike spikelet pair density (*CSD*), primary branch spikelet pair density (*PSD*), tassel branch angle (*TBA*), and tassel weight (*TW*) measured in three or four environments

Parameters	Entries (no)	L1[a] (cm)	L2 (cm)	TBN (no)	CSD[b] (no)	PSD (no)	TBA (degrees)	TW (g)
Means[c]								
IHO	1	29.9 ± 0.15	16.0 ± 2.59	30.0 ± 7.55	34.0 ± 4.24	24.7 ± 0.21	25.0 ± 7.07	8.68 ± 2.51
B73	1	27.8 ± 2.48	18.8 ± 2.27	8.05 ± 0.65	27.8 ± 1.70	13.1 ± 2.09	72.0 ± 7.07	2.14 ± 0.23
BC_1S_1	150	32.2 ± 0.87	22.3 ± 0.74	10.6 ± 0.89	26.9 ± 1.76	13.6 ± 0.97	61.5 ± 3.92	3.00 ± 0.25
Variance components (BC_1S_1 lines)								
$\hat{\sigma}^2_g$		0.84 ± 0.19**	0.58 ± 0.13**	1.52 ± 0.27**	1.90 ± 0.63**	0.63 ± 0.20**	8.87 ± 3.05**	0.08 ± 0.02**
$\hat{\sigma}^2_{ge}$		0.80 ± 0.24**	0.60 ± 0.17**	1.36 ± 0.23**	2.66 ± 0.89**	0.25 ± 0.30**	23.9 ± 4.05**	0.11 ± 0.02**
$\hat{\sigma}^2$		4.47 ± 0.27**	3.18 ± 0.19**	3.55 ± 0.21**	13.3 ± 0.91**	5.20 ± 0.35**	44.4 ± 2.99**	0.29 ± 0.02**
Heritability (BC_1S_1 lines)								
$\hat{h}^2$		0.52	0.51	0.66	0.38	0.40	0.37	0.57
90% C.I. on $\hat{h}^2$		(0.38 ; 0.63)	(0.36 ; 0.62)	(0.55 ; 0.74)	(0.17 ; 0.53)	(0.20 ; 0.54)	(0.16 ; 0.52)	(0.43 ; 0.67)

[a] L1, L2, TBN, and TW were measured in four environments: 1996, 2001–2003

[b] CSD, PSD, and TBA were measured in three environments: 2001–2003

[c] Standard errors are attached

Phenotypic and genotypic variances were highly significant ($P < 0.01$) for all traits. Estimates of $\hat{\sigma}^2_{ge}$ were significantly ($P < 0.01$) greater than zero for all traits. Heritability estimates ($\hat{h}^2$) for directly measured tassel traits ranged from 0.37 for TBA to 0.66 for branch number (Table 2). For calculated traits $\hat{h}^2$ ranged from 0.31 for the total number of spikelet pairs on central spike to 0.66 for the ratio branch number/L2 (Table 3). Genotypic correlations were significant and of intermediate magnitude for most trait combinations (Table 4).

Principal component analysis

Principal Component1 had an eigenvalue (λ) of 5.7 and explained 40% of the total variation present in the

Table 3 Means of parents Illinois High Oil (*IHO*) and B73, and 150 S_1 lines derived from backcross (IHO × B73) B73, along with estimates of variance components and heritabilities among BC_1S_1 families for calculated traits, including branch zone length (*L3*), total spikelet pairs on central spike (*TS*), ratio of primary tassel branch number to central spike length (*TBN*/*L2*), primary branch density (*TBN*/*L3*), ratio of short-branch meristems to long-branch meristems (*TS*/*TBN*), and ratio of branch zone length to central spike length (*L3*/*L2*) measured in three or four environments

Parameters	Entries (No)	L3[a] (cm)	TS[b] (cm)	TBN/L2 (cm^{-1})	TBN/L3 (cm^{-1})	TS/TBN	L3/L2
Means[c]							
IHO	1	14.0 ± 2.70	169.9 ± 22	2.14 ± 0.92	2.21 ± 0.28	10.2 ± 2.69	1.02 ± 0.42
B73	1	9.04 ± 1.03	152.8 ± 13	0.44 ± 0.07	0.90 ± 0.06	21.9 ± 0.68	0.50 ± 0.07
BC_1S_1	150	9.90 ± 0.56	153.1 ± 11	0.49 ± 0.05	1.09 ± 0.10	15.8 ± 1.83	0.45 ± 0.03
Variance components (BC_1S_1 lines)							
$\hat{\sigma}^2_g$		0.39 ± 0.08**	52.7 ± 22.1**	0.00[d] ± 0.00**[e]	0.01 ± 0.00**	2.19 ± 0.69**	0.00 ± 0.00**
$\hat{\sigma}^2_{ge}$		0.34 ± 0.10**	71.0 ± 35.4**	0.00 ± 0.00**	0.01 ± 0.00**	3.50 ± 0.95**	0.00 ± 0.00**
$\hat{\sigma}^2$		1.83 ± 0.11**	575.8 ± 39.6**	0.01 ± 0.00**	0.04 ± 0.00**	13.1 ± 0.93**	0.01 ± 0.00**
Heritability (BC_1S_1 lines)							
$\hat{h}^2$		0.55	0.31	0.66	0.50	0.40	0.57
90% C.I. on $\hat{h}^2$		(0.41; 0.65)	(0.08; 0.47)	(0.55; 0.74)	(0.34; 0.61)	(0.20; 0.54)	(0.44; 0.67)

[a] L3, TBN/L2, TBN/L3, and L3/L2 were calculated in four environments: 1996, 2001–2003

[b] TS and TS/TBN were calculated in three environments: 2001–2003

[c] Standard errors are attached

[d] Varaince was less than 0.01

[e] Standard error less than 0.01

Table 4 Phenotypic (r_p, upper diagonal) and genotypic (r_g, lower diagonal) correlation coefficients among tassel characteristics calculated in a population of 150 S_1 families derived from backcross (IHO × B73) B73

	Traits												
	L1	L2	L3	TBN	TBA	TW	CSD	PSD	TS	TS/TBN	TBN/L2	TBN/L3	L3/L2
L1		0.78**	0.55**	0.07	–0.06	0.36**	–0.34**	–0.18*	0.12	0.01	–0.21*	–0.30**	0.09
L2	0.79[b]		–0.09	–0.24**	–0.13	0.29**	–0.18*	–0.10	0.39**	0.39**	–0.54**	–0.22**	–0.54**
L3	0.47[b]	–0.16		0.46**	0.06	0.20*	–0.33**	–0.16*	–0.35**	–0.55**	0.42**	–0.20*	0.88**
TBN	0.11	–0.27[a]	0.63[b]		–0.35**	0.56**	0.15	0.29**	0.02	–0.81**	0.94**	0.78**	0.49**
TBA	–0.11	–0.20	0.12	–0.52[b]		–0.37**	–0.32**	–0.22**	–0.37**	0.07	–0.23**	–0.42**	0.10
TW	0.39[a]	0.35[a]	0.08	0.61[b]	–0.59[b]		0.13	0.33**	0.28**	–0.27**	0.37**	0.45**	0.04
CSD	–0.57[b]	–0.18	–0.76[b]	0.14	–0.80[b]	–0.03		0.51**	0.83**	0.33**	0.21*	0.41**	–0.21*
PSD	–0.26[a]	–0.03	–0.41[a]	0.58[b]	–0.52[b]	0.57[b]	0.62[b]		0.40**	–0.03	0.30**	0.45**	0.09
TS	–0.04	0.43[a]	–0.78[b]	–0.06	–0.88[b]	0.12	0.81[b]	0.50[b]		0.54**	–0.11	0.25**	–0.49**
TS/TBN	–0.11	0.35[b]	–0.87[b]	–0.85[b]	0.00	–0.38[b]	0.28	–0.31[a]	0.54[b]		–0.84**	–0.49**	0.66**
TBN/L2	–0.20[a]	–0.57[b]	0.61[b]	0.95[b]	–0.37[a]	0.42[b]	0.23[a]	0.56[b]	–0.18	–0.86[b]		0.74**	0.62**
TBN/L3	–0.12	–0.17	0.08	0.83[b]	–0.70[b]	0.66[b]	0.62[b]	0.98[b]	0.43[a]	–0.46[b]	0.77[b]		–0.07
L3/L2	0.03	–0.59[b]	0.90[b]	0.58[b]	0.19	–0.09	–0.56[b]	–0.30[a]	–0.86[b]	–0.84[b]	0.73[b]	0.13	

*, ** Phenotypic correlation was significant at the 0.05 and 0.01 probability level, respectively

[a,b] Genetic correlation exceeded one or two times its standard error, respectively

L1 total tassel length, *L2* central spike length, *L3* branch zone length, *TBN* tassel branch number, *TBA* tassel branch angle, *TW* tassel weight, *CSD* central spike spikelet pair density, *PSD* primary branch spikelet pair meristem density, *TS* total spikelets on central spike, *TS/TBN* total spikelets on central spike/branch number, *TBN/L2* branch number/central spike length, *TBN/L3* primary branch density, and *L3/L2* branch zone length/central spike length

dataset. For PC1 the loadings of TBN, TBN density, the ratio of short-branch meristems (spikelets) to long-branch meristems (tassel branches), and ratio of TBN to L2 were substantial (i.e., –0.30 > loadings > 0.30, Table 5). PC2 accounted for 25% of the variation and had a λ of 3.5. For PC2 the loadings of spikelet density on central spike, primary (long) branch spikelet density, and total spikelets on central spike (TS) were also substantial. The λ of PC3 was 2.4, and PC3 explained 17% of the variation. The loadings of L1, L2, and TW were the highest in this group.

Table 5 Parameters associated with the first three PCs and their loadings

Parameter	PC1	PC2	PC3
Eigenvalue (λ)	5.7	3.5	2.4
Total variation (%)	40.0	25.0	16.5
Heritability ($\hat{h}^2$)[a]	0.13	0.30	0.11
Trait loadings			
Total tassel length	0.00	0.00	**0.62**
Central spike length	–0.16	0.15	**0.55**
Branch zone length	0.26	–0.30	0.25
Tassel branch number	**0.40**[b]	0.11	0.00
Tassel branch angle	–0.17	–0.27	–0.12
Tassel Weight	0.25	0.25	**0.32**
Central spike spikelet density	0.00	**0.38**	–0.28
Primary branch spikelet density	0.13	**0.32**	–0.13
Total spikelets on central spike	0.00	**0.46**	0.00
Ratio of total spikelets on central spike to branch number	**–0.38**	0.11	0.00
Ratio of branch number to central spike length	**0.46**	0.00	0.00
Tassel branch number density	**0.33**	0.27	0.00
Ratio of branch zone length to central spike length	0.23	–0.25	0.00

[a] Heritability of PCs were calculated by performing PCA on correlation matrix of plot means of each replicate

[b] PC loadings larger than 0.30 and smaller than –0.30 were regarded as substantial

Single trait quantitative trait loci analysis

Two QTL explaining a total of 40.5% of $\hat{\sigma}_g^2$ on chromosomes 5 and 7 were found to affect primary TBN (Table 6). The QTL in bin 7.02 explained 16.7% of $\hat{\sigma}_p^2$, whereas the other in bin 5.06 explained 14.3% of $\hat{\sigma}_p^2$. Four QTL explaining a total of 63.1% of $\hat{\sigma}_g^2$ on chromosomes 1, 2, 4, and 9, were detected for spikelet pair density on central spike. Four QTL involved in inheritance of spikelet pair density on primary branches were identified on chromosomes 1, 4, 5, and 9 and explained a total of 64.4% of $\hat{\sigma}_g^2$. The QTL in bin 9.02 accounted for 13.5% of $\hat{\sigma}_p^2$ while the other QTL explained between 8.2 and 9.4% of $\hat{\sigma}_p^2$.

The QTL model for TW included six QTL on chromosomes 1, 3–5, 7, and 9 and accounted for 72.3% of total $\hat{\sigma}_g^2$. The QTL in bin 7.02 explained 13.3% of $\hat{\sigma}_p^2$ while the other QTL explained between 8.0 and 12.7% of $\hat{\sigma}_p^2$. Two QTL were detected for TBA on chromosomes 5 and 9 and explained 39.5% of $\hat{\sigma}_g^2$. For L1, we found five QTL on chromosomes 1, 4–7, which

Table 6 Parameters associated with QTL for primary tassel traits estimated from 150 S_1 families derived from backcross (IHO × B73) B73

Trait	Bin[a]	QTL Position[b]	Marker interval	Support interval	LOD	QTL effect[c]	Partial R^{2d}
Total tassel length	1.10	134	umc106–bmc1671	122–136	3.13	0.46 cm	13.8
	4.05	42	umc1662–umc2284	36–46	5.22	0.28 cm	5.5
	5.02/5.03	94	phi113–p150018	84–98	4.10	0.30 cm	6.3
	6.06/6.07	164	dup015–umc62	154–164	3.20	–0.26 cm	5.2
	7.02	24	gl1–dup009	20–28	4.69	–0.42 cm	10.0
							P^e = 50.9%
Central spike length	3.05/3.06	38	n204–bmc1047	30–44	4.47	–0.29 cm	4.5
	10.02	22	bmc1451–phi059	16–34	3.72	0.29 cm	5.5
							P = 13.0%
Tassel branch number	5.06/5.07	166	p200531–phi048	158–168	4.63	–0.83(#)	14.3
	7.02	0	phi034–ra1	0–4	6.19	–0.82(#)	16.7
							P=40.5%
TBA	5.04	102	co7bo2cd–p100014	96–110	6.12	1.28°	11.2
	9.02/9.03	36	bnlg244–phi037	20–42	2.67	1.04°	8.1
							P=39.5%
Tassel Weight	1.10	128	umc106–bmc1671	116–136	4.53	0.16 g	12.7
	3.07/3.06	60	bmc1605–bnlg197	58–76	4.25	–0.14 g	11.2
	4.03	0	bmc1126–nc004c	0–4	3.40	–0.11 g	8.0
	5.06/5.07	168	p200531–phi048	160–168	3.90	–0.14 g	10.0
	7.02	0	phi034–ra1	0–2	6.38	–0.17 g	13.3
	9.02	30	phi017–bnlg244	18–42	4.14	–0.15 g	10.7
							P=72.3%
Central spikelet pair density	1.06	40	n279–umc67	36–54	5.14	–0.45(#)	9.6
	2.04	10	phi083–umc14	0–20	5.08	0.45(#)	7.5
	4.08	92	n410–bnlg292	86–98	3.28	0.40(#)	7.7
	9.02	34	phi017–bnlg244	28–40	3.79	–0.44(#)	9.5
							P=63.1%
Primary branch spikelet pair density	1.05/1.06	34	umc167–n279	26–40	5.32	–0.25(#)	8.2
	4.05	42	umc1662–umc2284	36–50	4.03	–0.25(#)	8.7
	5.04	104	co7bo2cd–p100014	94–116	3.16	–0.28(#)	9.4
	9.02/9.03	38	bnlg244–phi027	34–46	4.69	–0.32(#)	13.5
							P=64.4%

[a] Bin number of left flanking marker, taken from Maize GDB

[b] QTL position in cM from the top of the chromosome as calculated by PLABQTL

[c] The additive effect of each QTL is calculated as the average effect of substituting the allele from parent P1 (B73) by the allele from P2 (IHO). Therefore, positive values indicate that B73 carries the allele for an increase in the trait, and negative values indicate that IHO contributes the alleles for an increase in the trait

[d] Proportion of phenotypic variation accounted for each QTL calculated by multiple regression in PLABQTL

[e] Proportion of adjusted genotypic variation explained by the final model

explained 50.9% of total $\hat{\sigma}_g^2$. The QTL in bin 1.10 explained 13.8% of $\hat{\sigma}_p^2$, whereas the other QTL explained between 5.2 and 10.0% of $\hat{\sigma}_p^2$. Two QTL on chromosomes 3 and 10 were identified for L2 and they explained a total of 13% of $\hat{\sigma}_g^2$.

Among the calculated traits, we identified four QTL on chromosomes 2, 4, 8, and 9 for total spikelet pairs on central spike, which explained a total of 82.8% of $\hat{\sigma}_g^2$ (Table 7). Four QTL explaining a total of 66% of $\hat{\sigma}_g^2$ on chromosomes 1, 4, 7, and 8 were detected for L3. The LOD scores ranged from 3.42 in bin 4.09 to 12.66 in bin 7.02. The latter QTL explained 28.3% of $\hat{\sigma}_p^2$, while the other QTL explained between 8.4 and 12.8% of $\hat{\sigma}_p^2$. For the ratio short-branch meristems to long-branch meristems three QTL on chromosomes 4, 6, and 7 were identified, which explained a total of 56.1% of $\hat{\sigma}_g^2$. For the ratio branch number to L2, we detected two QTL on chromosomes 5 and 7, each explaining 12.0 and 17.2% of $\hat{\sigma}_p^2$, respectively. For primary branch number density three QTL explaining a total of 55.1% of $\hat{\sigma}_g^2$ were found on chromosomes 3, 5, and 8.

Comparison across traits

Based on marker intervals, QTL of all 13 traits can be summarized as 24 different QTL regions, 11 of which were common for two or more traits (see Fig. 2). The

Table 7 Parameters associated with QTL for calculated tassel traits estimated from 150

Trait	Bin[a]	QTL Position[b]	Marker interval	Support interval	LOD	QTL effect[c]	Partial R^{2d}
Branch zone length	1.10	136	umc106–bmc1671	128–136	4.37	0.27 cm	12.8
	4.09	94	bnlg292–umc1101	88–100	3.42	–0.23 cm	8.4
	7.02	0	phi034–ra1	0–4	12.66	–0.44 cm	28.3
	8.02/8.03	18	n260–bmc2235	8–28	3.59	0.27 cm	10.8
							P^e = 65.3%
Total spikelet pairs on central spike	2.04	6	phi083–umc14	0–18	3.61	2.18(#)	7.3
	4.08	92	n410–bnlg292	86–100	2.99	2.11(#)	8.4
	8.03/8.05	58	bmc1834–umc1130	48–66	3.07	–2.14(#)	7.0
	9.02	34	phi017–bnlg244	28–40	3.02	–2.30(#)	9.9
							P = 82.8%
Short branch mersitems/ long branch meristems	4.08	92	bmc2244–n410	88–98	6.76	0.65	14.9
	6.05	146	phi129–dup015	122–152	2.68	–0.35	5.0
	7.02	0	phi034–ra1	0–6	3.77	0.50	10.2
							P = 56.1%
Branch number/central spike length	5.06/5.07	164	p200531–phi048	156–168	4.25	–0.04 cm^{-1}	12.0
	7.02	2	phi034–ra1	0–6	7.10	–0.04 cm^{-1}	17.2
							P = 52.2%
Primary branch density	3.08	90	n432–n457	80–102	2.72	–0.04	6.1
	5.04	100	co7bo2cd–p100014	96–106	4.52	–0.05	8.0
	8.03/8.05	50	bmc1834–umc1130	44–60	3.07	–0.04	6.1
							P = 55.1%
Branch zone length/central spike length	4.08	92	n410–bnlg292	88–100	3.40	–0.10	9.1
	7.02	2	phi034–ra1	0–6	9.24	-0.03	24.1
	8.02	22	bmc2235–umc103	6–30	3.18	0.01	7.6
	10.02	22	bmc1451–phi059	10–32	2.71	–0.01	7.2
							P = 55.8%

[a] Bin number of left flanking marker, taken from Maize GDB

[b] QTL position in cM from the top of the chromosome as calculated by PLABQTL

[c] The additive effect of each QTL is calculated as the average effect of substituting the allele from parent P1 (B73) by the allele from P2 (IHO). Therefore, positive values indicate that B73 carries the allele for an increase in the trait, and negative values indicate that IHO contributes the alleles for an increase in the trait

[d] Proportion of phenotypic variation accounted for each QTL calculated by multiple regression in PLABQTL

[e] Proportion of adjusted genotypic variation explained by the final model

interval phi034-ra1 on chromosome 7 was significantly associated with six traits: branch number, L3, ratio L3 to L2, ratio branch number to L2, ratio TS to branch number, and TW. Central spike spikelet density, TS, the ratio TS to branch number, and the ratio L3 to L2 shared a common QTL on chromosome 4. Two marker intervals on chromosome 5 (co7bo2cd–p100014 and p200531–phi048) were each significant for three different traits. The interval co7bo2cd–p100014 was significant for TBA, primary branch spikelet density, and primary branch number density while the interval p200531–phi048 was significant for branch number, the ratio branch number to L2, and TW. On chromosome 9 common QTL were detected for central spike spikelet density, TS, and TW in marker interval phi017–bnlg244.

Principal component quantitative trait loci analysis

We found QTL for the first three PCs (Table 8). For PC1, we identified two QTL on chromosomes 4 and 7. The QTL in bin 7.02 explained 17.3% of $\hat{\sigma}_p^2$, while the other two QTL explained 6.9% of $\hat{\sigma}_p^2$. For PC2 we detected four QTL on chromosomes 4, 5, 8, and 9. The QTL in bin 9.02 explained 14.6% of $\hat{\sigma}_p^2$, whereas the other QTL explained between 6.8 and 11.0% of $\hat{\sigma}_p^2$. Two QTL on chromosomes 1 and 2 were detected for PC3, which explained 9.7 and 2.6% of $\hat{\sigma}_p^2$, respectively.

Discussion

Our analyses revealed relationships among different inflorescence architecture traits, which is relevant to efforts for manipulating multiple traits. Tassel branch angle is a tassel architecture trait that influences pollen dispersal. We observed significant negative correlations between TBA and branch number, central spike spikelet density, and primary branch spikelet density. We also observed negative correlations between TBA and TBN, central spike spikelet density, and primary branch spikelet density in the (ILP × B73) B73 pop-

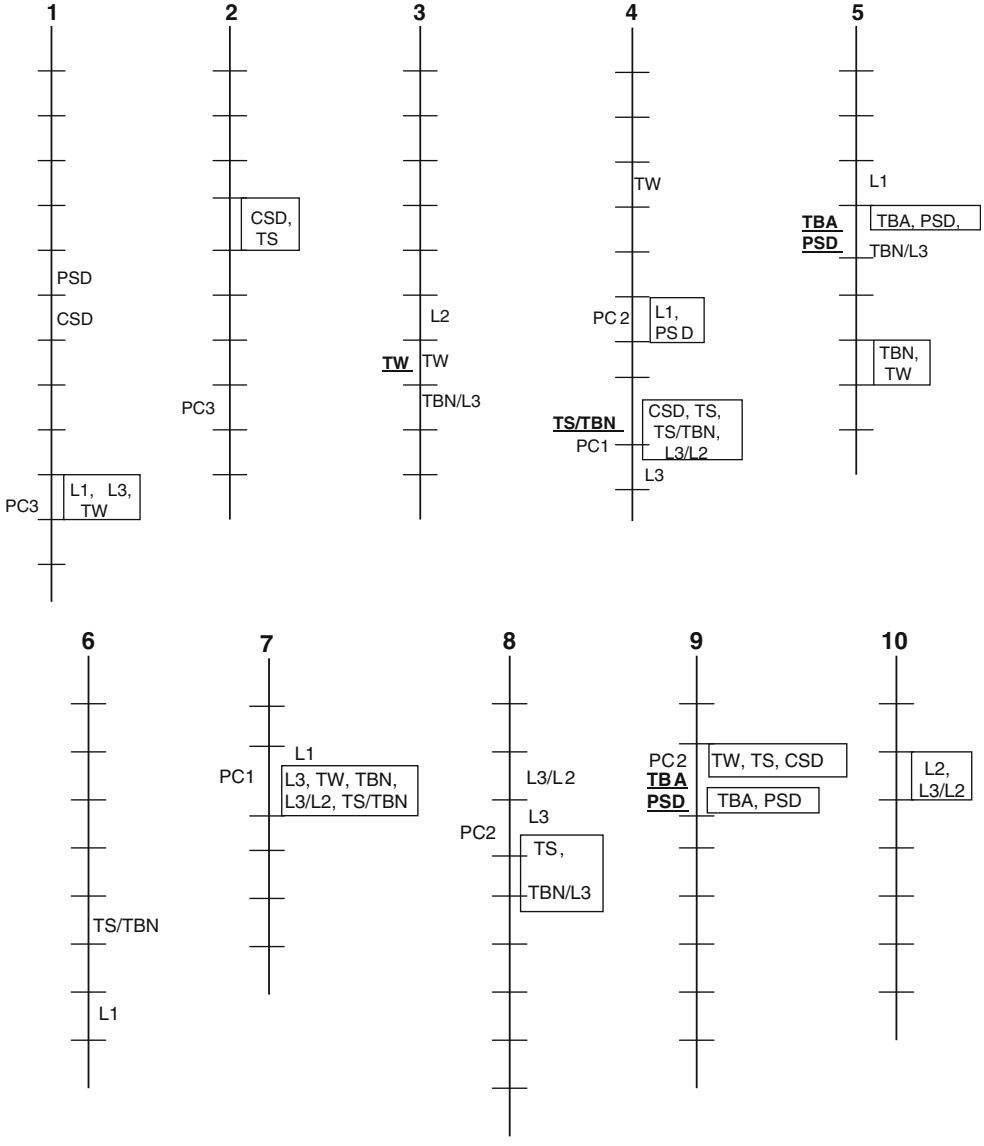

Fig. 2 Chromosomal positions of univariate QTL are right of chromosome and PC QTL are *left* of chromosome for the 150 S_1 families derived from (IHO × B73) B73. Each chromosome is divided into bins, with the first bin being bin 0. QTL congruent with (ILP × B73) B73 S_1 population (based on same bin) are *left* of chromosome indicated by *bold* and *underlined letters*. *L1* total tassel length, *L2* central spike length, *L3* branch zone length, *TBN* tassel branch number, *TBA* tassel branch angle, *TW* tassel weight, *CSD* central spike spikelet pair density, *PSD* primary branch spikelet pair meristem density, *TS* total spikelets on central spike, *TS/TBN* total spikelets on central spike/ tassel branch number, *TBN/ L2* tassel branch number/ central spike length; *TBN/L3* primary branch number density, and *L3/L2* branch zone length/central spike length

Table 8 Parameters associated with QTL for the first three PCs, derived from all the 13 tassel traits, estimated from 150

Principal Component	Bin[a]	QTL Position[b]	Marker interval	Support interval	LOD	Partial R^{2c}
PC1	4.09	96	bnlg292–umc1101	92–108	2.53	6.9
	7.02	2	phi034–ra1	0–6	8.19	17.3
PC2	4.06	44	umc2284–bmc2291	38–50	3.67	6.8
	5.04/5.06	128	p100014–p200531	118–138	6.02	7.5
	8.03	54	bmc1834–umc1130	44–64	2.90	11.0
	9.02	36	bnlg244–phi027	30–40	5.59	14.6
PC3	1.10	130	umc106–bmc1671	114–136	4.95	9.7
	2.08	40	n298–phi127	38–40	3.45	2.6

[a] Bin number of left flanking marker, taken from Maize GDB

[b] QTL position in cM from the top of the chromosome as calculated by PLABQTL

[c] Proportion of phenotypic variation accounted for each QTL calculated by multiple regression in PLABQTL

ulation (Upadyayula et al. 2006). However, this correlation could be expected in part due to architecture similarities in both donor parents ILP and IHO. These cultivars are characterized by lower TBAs (ILP, 32° and IHO, 25°) with numerous branches (ILP, 21.5 and IHO, 30.0) and high-spikelet density on central spike (ILP, 33.53 and IHO, 34.0) and primary branches (ILP, 21.7 and IHO, 24.7). This is in contrast to B73 that has upright tassels, fewer branches and lower spikelet densities (Table 2).

For most QTL experiments, multiple correlated traits are under study, and results often suggest that several traits are influenced by the same or linked loci. Most breeding programs strive to improve several traits simultaneously. Identification of QTL influencing multiple traits could increase the efficiency of marker assisted selection and enhance genetic progress. Multivariate approaches have been proposed by several authors to increase the power of QTL detection and to test hypotheses involving multiple traits (Jiang and Zeng 1995; Korol et al. 1995). Although multivariate approaches have several advantages over univariate analysis care should be taken not to include too many traits in the model. In multivariate analysis, a set of parameters is estimated for each trait. Thus when the number of traits in the model increases, so does the number of parameters to be estimated and as a result the power and precision of multivariate analysis decreases (Stearns et al. 2005). However, PCA allows for multiple traits to be analyzed without an increase in the number of parameters to be estimated as traits are combined into single orthogonal PCs that can be analyzed with univariate methods.

Based on inspection for the highest loading values for individual traits within PCA, variation of tassel architecture can be partially classified into three major groups: (1) long-branch meristems (tassel branches), (2) short-branch meristems (spikelets), and (3) tassel lengths. PC1 appears to largely represent variation in number of long-branch meristems and ratios with short-branch meristems, L2 and L3 (Table 5). The interval phi034-ra1 on chromosome 7 (bin 7.02) explained 17.3 of σ_p^2 for PC1. This interval, as expected, was also significant for individual traits: branch number (explaining 16.7% of σ_p^2), ratio of short-branch meristems to long-branch meristems (explaining 10.2% of σ_p^2), L3 (explaining 28.3% of σ_p^2), ratio of branch number and L2 (explaining 17.2% of σ_p^2), and TW (explaining 13.3% of σ_p^2). Expression of *ramosa1* (*ra1*) is known to impose short-branch meristems as long-branch meristems are initiated (Vollbrecht et al. 2005), making *ra1* a logical candidate gene for regulating the quantitative transition from long-branch meristems to short-branch mersitems, which would effect a number of inflorescence architecture traits. However, the peak of the QTL in all estimates for all significantly associated traits is at or near phi034 and the confidence interval of the QTL in all cases does not encompass *ra1*. Further research is warranted to identify the gene or genes underlying the QTL in the phi034-ra1 interval. A larger population size and/or a random mated population will increase precision of QTL mapping (Laurie et al. 2004). A complementary approach to identify the causal gene(s) will be to perform association analysis (Remington et al. 2001) using *ra1* and other putative candidate genes located in this interval.

Quantitative trait loci were detected for PC2, which were largely involved in production of short branch meristems. The QTL with largest effects for PC2 was detected in bin 9.02, explaining 14.6% of $\sigma^2{}_p$. We detected QTL for several traits in another mapping population (Upadyayula et al. 2006) in the same region and, therefore, suspect that this region might be important for tassel inflorescence architecture. The interval umc2284–bmc2291 on chromosome 4 (bin 4.06) explained 6.8% of σ_p^2. These markers flank the *fasciated ear2* (*fea2*) locus. Plants carrying the *fea2* allele develop larger meristems during inflorescence and floral shoot development and have a more prominent ear inflorescence, suggesting that *fea2* normally acts to limit the extent of growth of all meristem types (Taguchi-Shiobara et al. 2001). *Fea2* also maps to the location of a QTL for TBN (Upadyayula et al. 2006) and seed row number, a measure of the number of vertical rows of seed on the ear (Veldboom and Lee 1994). Hence, it is potentially possible that non-mutant allelic variation at *fea2* could be manipulated to alter ear and tassel inflorescence architecture.

We detected QTL for PC2 in bins 4.06, 5.04–6, and for PC3 in bin 2.08 but we did not detect QTL in these intervals for any of the individual traits. Perhaps these QTL were detected because of increase in power of detection and these QTL might be involved in more overall regulation of short-branch meristems. The identification of ''PC exclusive QTL'' supports our approach to identify genomic regions that might be involved in regulation of multiple traits, which could not be detected using trait-by-trait analysis. The QTL for PC3 in bin 2.08 did not have any individual trait QTL in this bin or adjacent bins, notably the QTL identified for PC2 were close to some individual trait QTL, with one marker in common with individual trait intervals. The PC2 QTL in bin 4.06 (umc2284–bmc2291) is close to QTL for L1 and primary branch spikelet pair density (umc1662–umc2284). The PC2 QTL in bin 5.04–6 is close to QTL for TW and branch

number to L2 ratio (p200531–phi048) and a QTL for primary branch density (co7bo2cd–p100014). Therefore, information from both individual trait and PC QTL analysis should be considered collectively in future use of these results.

One useful aspect of QTL mapping is the congruency of QTL positions across different populations. We compared our QTL results with our previous study (Upadyayula et al. 2006) involving a similar set of tassel traits in (ILP × B73) derived mapping population. Both donor parents, ILP and IHO, originated from the same open pollinated cultivar 'Burr's White' and from 90th cycle of Illinois Long-Term selection (Dudley and Lambert 1992). However, they were selected for low protein and high-oil concentrations, respectively, and indirect selection or genetic drift resulted in some differences in tassel architecture. The criterion of overlapping bin regions used by Tuberosa et al. (2002) was used to declare the QTL congruent between populations for a specific trait. Two QTL in bins 5.04 and 9.02 were common for TBA and tassel branch spikelet density in both the populations (see Fig. 2). This suggests that TBA and tassel branch spikelet density may have common genetic control at these loci, which is supported by significant genetic correlations in both populations. The *thick tassel dwarf1* (*td1*) mutant, which is associated with increased spikelet density on the main rachis and primary branches (Bommert et al. 2005) maps to bin 5.04 and provides a logical candidate gene for the spikelet density QTL in this bin. We observe common QTL in bin 3.07 for TW and for ratio of short-branch meristems to long-branch meristems in bin 4.08. The correspondence of these QTL in two populations strengthens the likelihood that these regions control variation for the respective traits, and that they function in more than one genetic background. Since a small percentage (16.67%) of QTL was in common between the two populations, we speculate that genetic control of the tassel architecture may be different between ILP and IHO. This finding is in despite of the two strains originating 90 cycles earlier from the same common source population, Burr's White. However, one major bottleneck for comparing QTL across populations or to perform a QTL meta-analysis is the commonalty of markers used in various mapping populations. In order to overcome this problem and to unlock the potential of QTL meta-analysis for candidate gene identification, development of a more useful set of highly polymorphic and well-distributed molecular markers is warranted.

We detected a number of QTL in this study, some influencing a single tassel inflorescence architecture trait and others influencing more than one architecture trait. The number of inflorescence architecture traits influenced by a QTL appears related to the timing of expression of the QTL during inflorescence development relative to the structural organization of the tassel. For example the QTL in the bin 7.02 region influences branch number, so it is not surprising that it also influences ratio of L3 to L2, and ratio of TS to branch number. Some QTL map to chromosome regions with logical candidate genes, such as *fea2*, *td1*, and *ral*. However, most of the QTL do not map to known mutant loci, yet, these QTL explain the majority of the variation for quantitative variation in inflorescence architecture. Thus there are a number of unknown genes regulating inflorescence architecture that are not revealed by known mutant loci. The QTL mapping information therefore serves as an important piece of initial information that can be used in positional cloning efforts with the upcoming availability of the complete maize genome sequence.

Acknowledgments This research was supported by NSF Plant Genome Research Program Grant 0110189 on Genetic Regulation of Inflorescence Architecture of Maize. We thank E. Vollbrecht and R. Martienssen for sharing *ramosa1* sequence. We appreciate technical assistance of Chandra Paul, Jerry Chandler, and Don Roberts.

References

Berke T, Rocheford T (1995) Quantitative trait loci for flowering, plant and ear height, and kernel traits in maize. Crop Sci 35:1439–1443

Bommert P, Lunde C, Nardmann J, Volbrecht E, Running M, Jackson D, Hake S, Werr W (2005) Thick tassel dwarf1 encodes a putative maize ortholog of the Arabidopsis CLAVATA1 leucine-rich repeat receptor-like kinase. Development 132:1235–1245

Bortiri E, Chuck G, Vollbrecht E, Rocheford T, Martienssen R, Hake S (2006) ramosa2 encodes a lateral organ boundary domain protein that determines the fate of stem cells in branch meristems of maize. Plant Cell (In press)

Brown MB, Forsythe AB (1974) Robust tests for the equality of variances. J Am Stat Assoc 69:364–367

Churchill GA, Doerge RW (1994) Empirical threshold values for quantitative trait mapping. Genetics 138:963–971

Draper RW, Smith H (1981) Applied regression analysis. 2nd edn. Wiley, New York, p 307

Dudley JW (1994) Molecular markers in plant improvement-manipulation of genes affecting quantitative traits (vol 33, p. 663, 1993). Crop Sci 34:322

Dudley JW, Lambert RJ (1992) Ninety generations of selection for oil and protein in maize. Maydica 37:1–7

Dudley JW, Lambert RJ (2004) 100 Generations of selection for oil and protein in corn. Plant Breeding Rev 24(Pt 1):79–110

Dudley JW, Lambert RJ, Alexander DE (1974) Seventy generations of selection for oil and protein concentration in maize kernel. In: Dudley JW (eds) Seventy generations of selection for oil and protein in maize. Crop Sci Am Madison, WI, pp181–212

Duvick DN, Cassman KG (1999) Post-green revolution trends in yield potential of temperate maize in the North-Central United States. Crop Sci 39:1622–1630
Federer WT, Wolfinger RD (1988) SAS code for recovering intereffect information in experiments with incomplete blocks and lattice rectangle designs. Agron J 950:545–551
Gilbert H, Le Roy P (2003) Comparison of three multitrait methods for QTL detection. Genet Sel Evol 35:281–304
Haley CS, Knott SA (1992) A simple regression method for mapping quantitative trait loci in line crosses using flanking markers. Heredity 69:315–324
Hallauer AR, Miranda JB (1988) Quantitative genetics in maize breeding. Iowa State University Press, Ames
Hospital F, Moreau L, Lacoudre F, Charcosset A, Gallias A (1997) More on the efficiency of marker assisted selection. Theor Appl Genet 95:1181–1189
Jansen RC, Stam P (1994) High resolution of quantitative traits into multiple loci via interval mapping. Genetics 136:1447–1455
Jiang C, Zeng ZB (1995) Multiple trait analysis of genetic mapping for quantitative trait loci. Genetics 140:1111–1127
Jolliffe IT (1986) Principal component analysis. Springer Verlag, New York
Knapp SJ, Stroup WW, Ross WM (1985) Exact confidence intervals for heritability on a progeny mean basis. Crop Sci 25:192–194
Knott SA, Haley CS (2000) Multiple least squares for quantitative trait loci detection. Genetics 156:899–911
Korol AB, Ronin YI, Kirzhner VM (1995) Interval mapping of quantitative trait loci employing correlated trait complexes. Genetics 140:273–284
Lambert RJ (2001) High-oil corn hybrids. In: Hallauer AR (eds) specialty corns. CRC Press, Boca Raton, FL, pp 131–154
Lambert RJ, Johnson RR (1977) Leaf angle, tassel morphology, and the performance of maize hybrids. Crop Sci 18:499–502
Laurie CC, Chasalow SD, LeDeaux JR, McCarroll R, Bush D, Hauge B, Lai C, Clark D, Rocheford TR, Dudley JW (2004) The genetic architecture of oil concentration in the maize kernel after 70 generations of divergent selection. Genetics 168:2141–2155
MaizeGDB (2006) The community database for maize genetics and genomics . http://www.maizegdb.org/; verified 5 January 2006
McSteen P, Laudencia-Chingcuanco D, Colasanti J (2000) A floret by any other name: control of meristem identity in maize. Trend Plant Sci 5:61–66
Mickelson SM, Stuber CS, Senior L, Kaeppler SM (2002) Quantitative trait loci controlling leaf and tassel traits in a B73 x Mo17 population of maize. Crop Sci 42:1902–1919
Mode CJ, Robinson HF (1959) Pleiotropism and genetic variance and covariance. Biometrics 15:518–537
Neuffer MG, Coe EH, Wessler SR (1997) Mutants of maize. Cold Spring Harbor Laboratory Press, Plainview, New York
Remington D, Thornsberry J, Matsuoka Y, Wilson L, Whitt S, Doebley J, Kresovich S, Goodman M, Buckler E (2001) Structure of linkage disequilibrium and phenotypic associations in the maize genome. Proc Natl Acad Sci USA. 98:11479–11484
Robertson DS (1985) A possible technique for isolating genic DNA for quantitative traits in plants. J Theor Biol 117:1–10
SAS Institute (2003) SAS proprietary software release 9.1. SAS Institute Inc., Cary, NC
Searle SR (1971) Linear models. Wiley, New York
Stearns TM, Beever JE, Southey BR, Ellis M, McKeith FK, Rodriguez-Zas SL (2005) Evaluation of approaches to detect quantitative trait loci for growth, carcass, and meat quality on swine chromosomes 2,6, 13, and 18. II. Multivariate and principal component analyses. J Anim Sci 83:2471–2481
Taguchi-Shiobara F, Yuan Z, Hake S, Jackson D (2001) The *fasciated ear2* gene encodes a leucine-rich repeat receptor-like protein that regulates shoot meristem proliferation in maize. Genes Dev 15:2755–2766
Tuberosa R, Sanguineti MC, Landi P, Giuliani MM, Salvi S, Conti S (2002) Identification of QTLs for root characteristics in maize grown in hydroponics and analysis of their overlap with QTLs for grain yield in the field at two water regimes. Plant Mol Biol 48:697–712
Upadyayula N, da Silva HS, Bohn MO, Rocheford TR (2006) Genetic and QTL analysis of maize tassel and ear architecture. Theor Appl Genet 112:592–606
Utz HF (2001) PLABSTAT: a computer program for statistical analysis of plant breeding experiments. http://www.uni-hohenheim.de/~ipspwww/soft.html; verified 25 May 2005
Utz HF, Melchinger AE (1996) PLABQTL: a program for composite interval mapping of QTL. http://www.uni-hohenheim.de/~ipspwww/soft.html; verified 25 May 2005
Van Ooijen JW, Voorrips RE (2001) JoinMap 3.0, Software for the calculation of genetic linkage maps. Plant Research International, Wageningen, the Netherlands
Veldboom LR, Lee M (1994) Molecular-marker-facilitated studies of morphological traits in maize. ÉÉ. Determination of QTLs for grain yield and yield components. Theor Appl Genet 89:451–458
Vollbrecht E, Springer P, Buckler E, Goh L, Martienssen RA (2005) Architecture of floral branch systems in maize and related grasses. Nature 436:1119–1126
Weller JI, Wiggans GR, VanRaden PM, Ron M (1996) Application of a canonical transformation to detection of quantitative trait loci with the aid of genetic markers in a multi-trait experiment. Theor Appl Genet 92:998–1002
Wilson L, Rinehart-Whitt S, Ibanez AM, Rocheford T, Goodman M, Buckler ES (2004) Dissection of maize kernel composition and starch production by candidate gene association. Plant Cell 16:2719–2733
Wych RD (1988) Production of hybrid seed corn. In: Sprague GF, Dudley JW (eds) Corn and corn improvement., American Society of Agronomy, Madison, WI
Zeng ZB (1994) Precision mapping of quantitative trait loci. Genetics 136:1457–1468